

Design of a Novel Inductive Non-Metallic Ultrasonic Emitting System

Chao Peng^{1,*}, Yue Song¹, Guangmin Zhang¹, Jincong Feng¹, Sha Zou²

¹School of Electrical Engineering and Intelligentization, Dongguan University of Technology, Dongguan, 523808, China

²School of Hengnan County Seventh Middle, Hengyang, 421000, China

*E-mail: pengchao@dgut.edu.cn

Keywords: Low-voltage ultrasonic transmitting system; Inductive ultrasonic transmission; Dual-core control system; Non-metallic ultrasonic flaw detection

Abstract: A new type of non-metallic ultrasonic transducer driving system is designed in this paper. Based on the analysis of the traditional ultrasonic transmitting circuit, a new type of ultrasonic transmitting circuit is designed by using the principle of inductance energy storage to generate high power pulse. The design uses the FET as the switching control component. Compared with the traditional capacitive ultrasonic transmitting system, the whole circuit design has the advantages of high security and no need to provide DC high voltage power supply. It also has the advantages of small size and easy adjustment of driving waveform parameters. The system outputs a trigger pulse signal through the two-core system to control the operating state of the entire circuit. By establishing the circuit model of the ultrasonic transmitting circuit and making the actual circuit, it is proved that the circuit can generate the ultrasonic pulse excitation signal with adjustable frequency and amplitude. Finally, experimental verification is carried out, the effect is good, and the hidden danger of safety is eliminated.

1. Introduction

Ultrasound is a kind of sound wave whose frequency is higher than 20,000 Hz. It has good direction, high power and is easy to obtain concentrated sound energy [1, 2]. These advantages make ultrasound widely used in ultrasonic testing [3, 4], ultrasonic processing and basic research related to ultrasound [5-7]. And ultrasonic detection involves ultrasonic detection, thickness measurement [8-10], ranging and medical ultrasound imaging [11-13]. The acoustic emission circuit is an important part of the ultrasonic flaw detector. The accuracy and stability of this part are essential for the entire ultrasonic flaw detection system [14, 15]. The non-metal detection transmitting circuit completes the excitation of the ultrasonic pulse signal, and the amount of excitation energy mainly depends on the voltage applied across the transducer [16]. Therefore, in order to get enough energy, it is necessary to generate a high voltage pulses.

Most of the high-voltage pulses are generated by the capacitor instantaneous discharge method. The capacitor instantaneous discharge method is mainly based on the principle that the voltage at both ends of the capacitor cannot be mutated at the beginning of charging and discharging. Charging process is the process of capacitor storage charge, discharge process is the process of capacitor release storage charge. The charging and discharging of the capacitor takes time. This is due to the charging and discharging process of the capacitor, which is essentially the process of accumulating and dissipating the charge on the capacitor. Since the change in the amount of charge takes time, charging and discharging also take time. At the beginning of charging, the charging current is larger and the voltage rises faster. With the increase of the voltage, the charging current decreases gradually, and the rising speed of the voltage becomes slower, which tends to approach the power supply voltage. Similarly, at the beginning of the discharge, the voltage and current changes are also faster, and later become slower. The capacitor transient transmitting circuit needs to provide stable DC high voltage. This high-voltage module will generally make the overall size of the transmitting circuit larger, higher cost, and there are potential safety hazards.

2. Analysis of the conventional ultrasonic transmitter circuit

Ultrasound emission system is an important part of the whole ultrasonic nondestructive testing system. The efficiency of ultrasonic flaw detection and the accuracy of final detection are closely related to the ultrasonic emission module. In recent years, the driving system of ultrasonic transducer mostly uses the pulse signal generated by the energy storage capacitor in the process of instantaneous charging and discharging to excite the ultrasonic transducer[17-19]. This kind of driving circuit is difficult to match impedance and tune voltage, and the DC high-voltage power supply is usually hundreds of volts, or even thousands of volts, which has potential high-voltage safety hazards. A conventional ultrasonic drive circuit is shown in Figure 1.

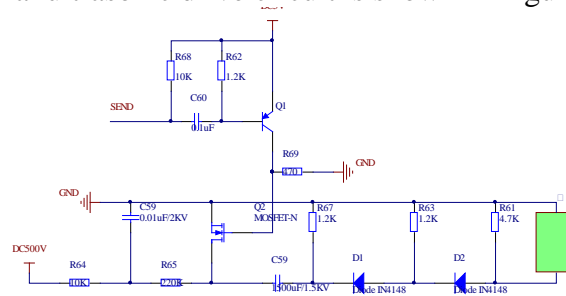


Figure 1 A conventional ultrasonic transmitting and driving circuit

The SEND signal in Figure 1 is a trigger pulse signal generated by the FPGA that controls the operating state of the entire circuit. The conduction and cut-off of MOS tube Q2 are controlled respectively by the high and low level of SEND signal. When the MOS transistor Q2 is in the off state, the DC high voltage power supply DC500V charges the capacitor C59 through R64 and R65. After charging is completed, the voltage across C59 is +500V. When the MOS is in the on-state, since the voltage across the capacitor cannot be suddenly changed, the two sections of the resistor R67 are clamped at -500V instantaneously, and discharged through Q2, R67, R63 and R61 to excite the probe to generate ultrasonic waves.

The above circuit has the following defects:

①Requirements for a stable DC high-voltage power supply, and this DC high-voltage power supply must be matched with the transmitter circuit part. At present, customized high-frequency transformer is commonly used, which brings the problems of large volume, long design cycle and high development cost to the whole transmitter system. At the same time, the high voltage of +500V will also bring a very large security risk.

②It is difficult to adjust the circuit parameters. Most of the above circuit diagrams are analog circuits, and there is no clear theoretical guidance for system parameter adjustment. If there are special requirements for the excitation signal of the probe, it is difficult to change the parameters of the drive circuit accordingly.

3. The overall design of the ultrasonic transmitting circuit

(1)Overall design of the system

The whole circuit of non-metallic ultrasonic transmitting circuit is shown in Figure 2. The whole system consists of four parts: ARM main control system, FPGA control system, square wave generator and inductance ultrasonic transmitting circuit. The main control system adopts the ARM+FPGA dual core composition to make the whole system more functional. The main control chip of ARM not only controls the emission control of the transmitting circuit by the FPGA, but also lays a solid foundation for the future expansion of the whole system. In addition to ensuring the accuracy of the overall system control, the control of the FPGA can also flexibly change the parameters of the transmitting system according to the requirements of the system.

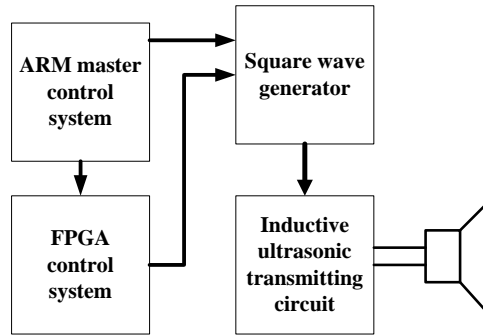


Figure 2 Overall block diagram of the system

(2)The design of the square wave generating circuit

The circuit shown in Figure 3 is a duty cycle adjustable pulse oscillation circuit composed of NE555, which is an improved circuit for the indirect feedback type unstable circuit[20]. The circuit includes a NE555 integrated chip U1, a resistor R1, a resistor R2, a sliding resistor RV1, a capacitor C1, a capacitor C2, and diodes D1 and D2 as switching elements. Pin 1 of NE555 is grounded, and NE555 pin 8 is connected to DC power supply +12V. Pin 3 of NE555 is a square wave output.

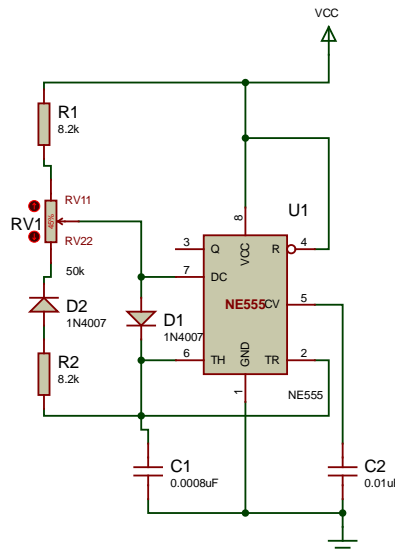


Figure 3 Square wave generator

As long as the voltage V_{cc} is applied to the circuit, the oscillator starts to oscillate. When the current is switched on, because the voltage on $C1$ can not mutate, that is, the starting level of pin 2 potential is ground potential, so that NE555 is set and the pin 3 is high. $C1$ charges it through the resistance of the upper half of $RAV1$ and $R1$. NE555 reset when the voltage on $C1$ is charged to the threshold level $2/3 V_{cc}$. When pin 3 turns to low level, $C1$ discharges through the lower half resistors of $R2$, $RV1$, $D2$ and NE555. If the duty cycle is D , the resistance of the first half of $RV1$ plus $R1$ is R_a , and the resistance of the second half of $RV1$ plus $R2$ is R_b , then the duty cycle can be set as follows:

$$D = \frac{T_1}{T} = \frac{R_a}{R_a + R_b} \quad (1)$$

When sliding resistor $RV1$ slides to the top, the duty cycle D can be calculated:

$$D = \frac{8.2}{8.2 + 8.2 + 50} \approx 12.3\% \quad (2)$$

When the sliding rheostat slides to the bottom, the duty ratio D can be calculated as:

$$D = \frac{8.2 + 50}{8.2 + 50 + 8.2} \approx 87.7\% \quad (3)$$

The frequency of square wave can be changed by adjusting capacitor C1, resistor R1, resistor R2 and sliding rheostat RV1 according to specific requirements. The specific formula is as shown in Equation 4:

$$F = \frac{1.443}{(R1 + R2 + RV1) \times C1} \quad (4)$$

(3) Design of inductive transmitting circuit

The specific circuit is shown in Figure 4. The circuit includes electrolytic capacitor C3, capacitor C4, diodes D3, D5, and Schottky diode D4. Resistors R3, R4, R5, R6, R7. With core inductor L1, inductor L2, N-channel enhanced power FET Q1. N-Channel Enhanced Power Field Effect Transistor Q1 is controlled by FPGA. Q1 is used as a switching element. It has two states: When the gate G input of Q1 is positive, Q1 is turned on. At this time, Q1 is equivalent to a very small resistor, which will be connected in series with the DC power supply +12V, the core inductor L1, and the resistor. Forming a circuit with a small resistance value, when the current value in the core inductor L1 rises rapidly for energy storage; When the gate G input of Q1 is negative, Q1 is switched off rapidly. At this time, the resonant circuit consisting of inductor L1, capacitor C4, resistor R6 and resistor R7 with iron core discharges rapidly, forming high voltage trigger pulse on resistor R7, which can reach hundreds of volts. Schottky diode D4 is characterized by a fast recovery speed, which is combined with the energy storage element to prevent sudden changes in voltage and current. Both poles D3 and D5 function as one-way switches. It should be specially noted that the resistor R6, the resistor R7 and the inductor L2 are connected in parallel to form a parallel matching circuit. The magnitude of the excitation pulse can be changed by adjusting the values of resistor R6 and resistor R7, while the value of sensor L2 can change the resonant frequency of the circuit and achieve the best driving effect.

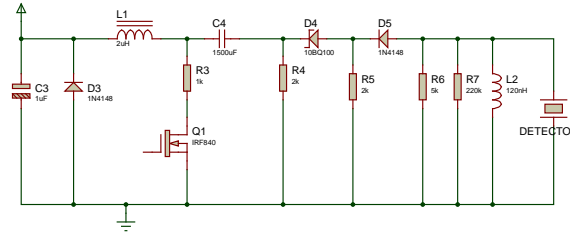


Figure 4 Inductive transmitting circuit

4. Experiment and test

After theoretically designing the circuit, we use PROTEL to simulate the whole circuit into a compact printed circuit board, and then make it into a physical object, as shown in Fig. 5. Then we tested the circuit. The test results are shown in Figure 6. We launched 520V ultrasonic probe excitation pulse. From the test results, the output waveform of the transmitting circuit is stable, the frequency is adjustable, and the pulse width and the excitation narrow pulse are in line with the engineering requirements of ultrasonic flaw detection.

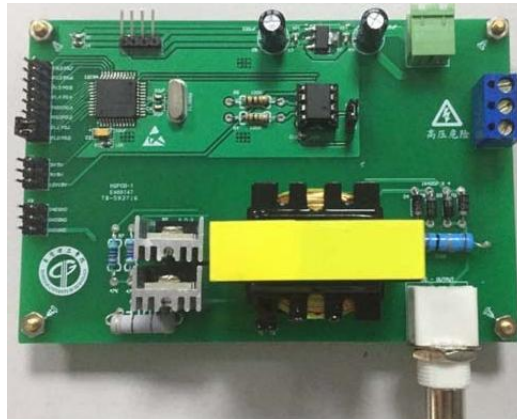


Figure 5 Physical map of the transmitting circuit



Figure 6 Excitation pulse waveform during test

It should be noted in the circuit designed in this paper that the control pulse width and the parameters of the capacitor roughly determine the pulse width of the emission. Transmitting power is a very important index of transmitting circuit. In the field of non-metallic ultrasonic testing, the thickness of the general detection is relatively thick, so a large transmission power is required. The transmit power can be calculated by Equation 5:

$$P = \frac{V^2 C}{t} \quad (5)$$

In formula 5, V is the instantaneous voltage on the capacitor when discharging, C is the capacitance, and t is the discharge time. When the whole transmitting circuit and the charging and discharging time are determined, the transmitting power is mainly determined by the instantaneous capacitance V and capacitance C when discharging. If the capacitance C is too large, it will affect the charging and discharging time. Therefore, increasing the emission voltage is the main way to increase the transmission power. At the same time, in order to obtain enough narrow pulse, the MOS tube should be shut down in time when capacitor discharge.

Another problem that should be paid attention to in the ultrasonic transmitting circuit is the determination of the radio frequency rate of the excitation pulse, i.e. the number of excitation pulses emitted per second. If the transmission frequency is too high, it will cause the transmitted signal that has not been sufficiently attenuated to enter the next cycle; Conversely, if the fruit is emitted too low, it will reduce the detection efficiency. Generally, in the field of non-metal detection, the excitation pulse has a transmission frequency of 100 Hz or more.

5. Conclusions

This paper proposes a non-metallic ultrasonic emission system different from the traditional capacitive instant method. It is an improved indirect feedback type unstable circuit composed of NE555. It can adjust the cycle of switching pulse very conveniently. At the same time, a new type of inductance ultrasonic transmitting circuit is designed, which is used as the excitation source of the ultrasonic probe through the principle that the core inductor of the energy storage element generates high voltage pulse in an instant, and the magnitude of the excitation pulse and the resonance frequency of the probe can be changed by adjusting the values of resistors and inductors. The overall designed circuit does not need to provide DC high voltage power supply, eliminating safety hazards, reducing the size of the transmitting circuit, reducing design cost and development cycle. The research of the thesis can provide technical support and theoretical guidance for ultrasonic nondestructive testing, and has certain engineering value.

Acknowledgements

This work was supported by Dongguan Municipal Science and Technology Bureau under grant No. 2016508140.

References

- [1] Benabbas, R., M. Hanna, J. Shah, and R. Sinert, Diagnostic Accuracy of History, Physical Examination, Laboratory Tests, and Point-of-care Ultrasound for Pediatric Acute Appendicitis in the Emergency Department: A Systematic Review and Meta-analysis. *Acad Emerg Med*, 2017. 24(5): p. 523-551.
- [2] Gress, F.G., The Early History of Interventional Endoscopic Ultrasound. *Gastrointest Endosc Clin N Am*, 2017. 27(4): p. 547-550.
- [3] Zhang, Y., C. Liao, H. Qu, S. Huang, H. Jiang, H. Zhou, E. Abrams, F.G. Habte, L. Yuan, E.H. Bertram, K.S. Lee, K.B. Pauly, P.S. Buckmaster, and M. Wintermark, Testing Different Combinations of Acoustic Pressure and Doses of Quinolinic Acid for Induction of Focal Neuron Loss in Mice Using Transcranial Low-Intensity Focused Ultrasound. *Ultrasound Med Biol*, 2018.
- [4] Fabiszewska, E., K. Pasicz, I. Grabska, W. Skrzynski, W. Slusarczyk-Kacprzyk, and W. Bulski, Evaluation of Imaging Parameters of Ultrasound Scanners: Baseline for Future Testing. *Pol J Radiol*, 2017. 82: p. 773-782.
- [5] Basaran, S., R. Has, I.H. Kalelioglu, B. Karaman, M. Kirgiz, T. Dehgan, B.N. Satkin, T.S. Sivrikoz, and A. Yuksel, Follow-Up Studies of cf-DNA Testing from 101 Consecutive Fetuses and Related Ultrasound Findings. *Ultraschall Med*, 2018.
- [6] Luo, S., D. Meng, Q. Li, X. Hu, Y. Chen, C. He, B. Xie, S. She, Y. Li, and C. Fu, Genetic Testing and Pregnancy Outcome Analysis of 362 Fetuses with Congenital Heart Disease Identified by Prenatal Ultrasound. *Arq Bras Cardiol*, 2018. 111(4): p. 571-577.
- [7] Tzartzeva, K. and A.G. Singal, Testing for AFP in combination with ultrasound improves early liver cancer detection. *Expert Rev Gastroenterol Hepatol*, 2018: p. 1-3.
- [8] Ng, K.W., A.R. Dietz, R. Johnson, M. Shoykhet, and C.M. Zaidman, Reliability of bedside ultrasound of limb and diaphragm muscle thickness in critically-ill children. *Muscle Nerve*, 2018.
- [9] Calvo-Lobo, C., I. Diez-Vega, M. Garcia-Mateos, J.J. Molina-Martin, G. Diaz-Urena, and D. Rodriguez-Sanz, Relationship of the skin and subcutaneous tissue thickness in the tensiomyography response: a novel ultrasound observational study. *Rev Assoc Med Bras (1992)*, 2018. 64(6): p. 549-553.
- [10] Storchle, P., W. Muller, M. Sengeis, S. Lackner, S. Holasek, and A. Furhapter-Rieger, Measurement of mean subcutaneous fat thickness: eight standardised ultrasound sites compared to 216 randomly selected sites. *Sci Rep*, 2018. 8(1): p. 16268.
- [11] Boucher, M.A., S. Lippe, C. Dupont, I.S. Knoth, G. Lopez, R. Shams, R. El-Jalbout, A. Dampousse, and S. Kadoury, Computer-aided lateral ventricular and brain volume measurements in 3D ultrasound for assessing growth trajectories in newborns and neonates. *Phys Med Biol*, 2018. 63(22): p. 225012.
- [12] Wang, X., Y. Gao, J. Li, J. Wu, B. Wang, X. Ma, J. Tian, M. Shen, and J. Wang, Diagnostic accuracy of endoscopic ultrasound, computed tomography, magnetic resonance imaging, and endorectal ultrasonography for detecting lymph node involvement in patients with rectal cancer: A protocol for an overview of systematic reviews. *Medicine (Baltimore)*, 2018. 97(43): p. e12899.
- [13] Shi, M., L. Ma, J. Zhang, and Q. Yan, Role of 25 MHz Ultrasound Biomicroscopy in the Detection of Subluxated Lenses. *J Ophthalmol*, 2018. 2018: p. 3760280.

- [14] Nguyen, L.T., G.K. Kocur and E.H. Saenger, Defect mapping in pipes by ultrasonic wavefield cross-correlation: A synthetic verification. *Ultrasonics*, 2018. 90: p. 153-165.
- [15] Song, Y., J.A. Turner, Z. Peng, C. Chao, and X. Li, Enhanced Ultrasonic Flaw Detection using an Ultra-high Gain and Time-dependent Threshold. *IEEE Trans Ultrason Ferroelectr Freq Control*, 2018.
- [16] Zhang, G., J. Zhu, Y. Song, C. Peng, and G. Song, A Time Reversal Based Pipeline Leakage Localization Method With the Adjustable Resolution. *IEEE Access*, 2018. 6: p. 26993-27000.
- [17] Tant, K.M., A.J. Mulholland and A. Gachagan, A model-based approach to crack sizing with ultrasonic arrays. *IEEE Trans Ultrason Ferroelectr Freq Control*, 2015. 62(5): p. 915-26.
- [18] Hu, P. and J.A. Turner, Contribution of double scattering in diffuse ultrasonic backscatter measurements. *J Acoust Soc Am*, 2015. 137(1): p. 321-34.
- [19] Benammar, A., R. Draï and A. Guessoum, Ultrasonic flaw detection using threshold modified S-transform. *Ultrasonics*, 2014. 54(2): p. 676-83.
- [20] Chen, P.K. and C.L. Lin, Synthesis of Genetic Clock with Combinational Biologic Circuits. *IEEE/ACM Trans Comput Biol Bioinform*, 2015. 12(5): p. 1206-12.